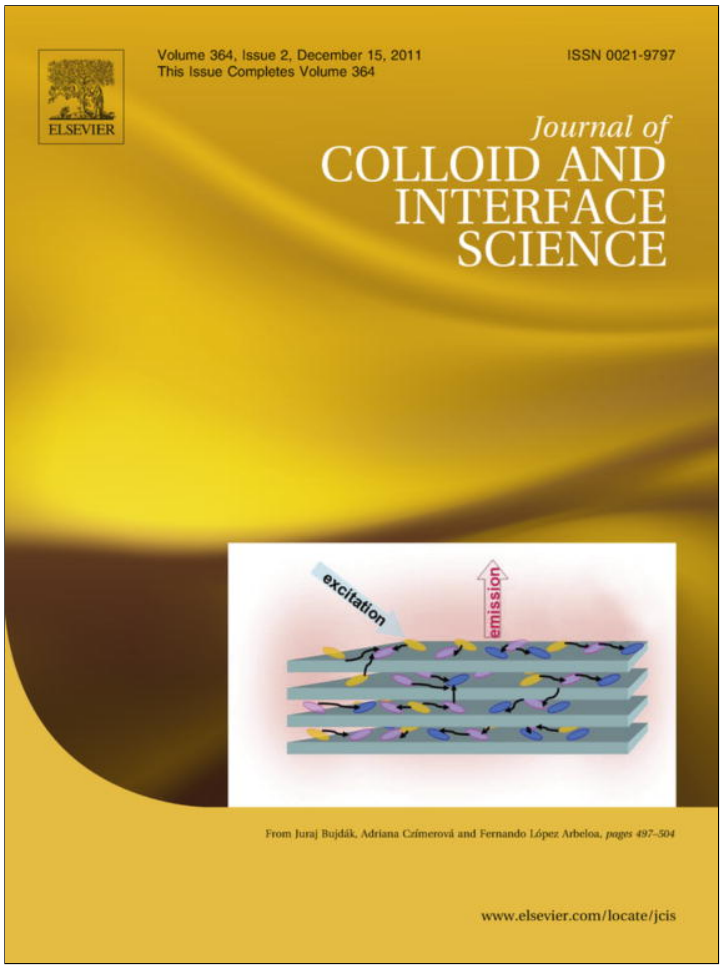

Journal of Colloid and Interface Science 364 (2011) 428–434

Contents lists available at SciVerse ScienceDirect

Journal of Colloid and Interface Science

www.elsevier.com/locate/jcis

Polydiacetylene-supported silica films formed at the air/water interface

Yelena Demikhovsky, Sofiya Kolusheva, Margarita Geyzer, Raz Jelinek *

Department of Chemistry and Ilse Katz Institute for Nanotechnology, Ben Gurion University, Beer Sheva 84105, Israel

ARTICLE INFO

Article history:
Received 23 July 2011
Accepted 28 August 2011
Available online 3 September 2011

Keywords:
Polydiacetylene
Mesostructured silica films
Color sensors
Free-standing thin films
Langmuir monolayers
Bacterial sensors

ABSTRACT

Mesostructured silica films have attracted interest as potential platforms for sensing, molecular sieving, catalysis, and others. The fabrication of free-standing silica films on water, however, is challenging due to the need for scaffolding agents that would constitute effective templates. We describe the assembly of thin film at the air/water interface comprising quaternary silicates and polydiacetylene (PDA), a unique chromatic polymer forming two-dimensional conjugated networks, and the use of these films for biological sensing. PDA exhibits a dual role in the system—both as the amphiphilic matrix facilitating immobilization of the silicate colloidal units at the air/water interface and additionally a chromatic reporter that undergoes visible blue–red transitions, accompanied by fluorescence transformations, in the presence of analytes. We demonstrate the application of the silicate/PDA thin films for the detection of bacterial proliferation.

1. Introduction

Mesostructured silica thin films have attracted interest due to their diverse structural properties as well as potential applications as molecular sieve membranes, catalysis supports, biomedicine, and platform for optoelectronic devices [1–4]. Silica thin film assemblies feature varied organizations, including lamellar and hexagonal mesostructures [5–7], and cubic phases [7]. Potential applicability of silica films requires uniform thickness and surface morphology, and even distribution of pores and molecular constituents [8,9]. Thin silica-based films have been grown from acidic solutions via evaporation-induced self-assembly methods such as spin coating [10,11] or via spontaneous growth at the air–liquid or solid–liquid interface [12,13].

The air/water interface, in particular, presents a unique low-dimensionality environment for the assembly of silica thin films. "Free-standing" mesoporous silica films have been reported to form spontaneously at the air/water interface [14]. The majority of such thin films have employed cationic surfactants such as cetyltrimethylammonium bromide (CTAB) which constitute a self-assembly "template" upon the water surface within which polymerized silica mesostructures form [15]. Polyelectrolytes such as polyethylenimine have been occasionally co-added to the surfactant/silica film mixture to achieve better organization of film microstructures [16]. While most studies of silica film growth at the air/water interface have focused on procedures employing cationic surfactants, *non-ionic* surfactants are generally cheaper, more environmentally friendly, and exhibit more diverse structural units [17]. Indeed, non-ionic surfactants have been widely used in matrixes for *bulk* mesoporous materials [18].

Here we describe the construction of thin films assembled from the mixtures of quaternary silica and *polydiacetylene* (PDA). PDA constitutes a conjugated ene–yne network produced upon ultraviolet polymerization of diacetylene monomers [19]. Since their introduction in the early 1970s, PDA systems, primarily vesicles and thin films, have attracted significant scientific and technological interest due to their unique chromatic properties [20–23]. Specifically, PDA matrixes undergo dramatic visible *colorimetric* and *fluorescence* transformations induced by diverse biological and chemical molecules and environmental factors, making PDA a potentially useful constituent in sensing platforms [24]. PDA films at the air/water interface (e.g., Langmuir films), in particular, have been studied extensively [25]. Such films exhibit interesting thermodynamic and structural properties [21,26] and have been also employed as chromatic sensing platforms [27]. Self-assembled films comprising PDA derivatives and hexagonal silica were produced through surface deposition and exhibited interesting chromatic properties [28]. In this study, we describe the assembly of mixed silica/PDA Langmuir films, characterization of their organization and physical properties both at the air/water interface as well as following transfer onto solid substrates, and their potential as a biosensing platform. We show that, in the mixed film systems, PDA constitutes both effective scaffolding for the assembly of interspersed silica colloids and a chromatic reporter for biological analytes.

* Corresponding author.
E-mail address: razj@bgu.ac.il (R. Jelinek).

0021-9797/$ - see front matter © 2011 Elsevier Inc. All rights reserved.
doi:10.1016/j.jcis.2011.08.078

2. Materials and methods

2.1. Materials

10,12-Tricosadiynoic acid (TRCDA) was purchased from Alfa Aesar. The compound was purified by dissolving the powder in chloroform and filtered through a 0.45 μm nylon filter. Purified powder was obtained by evaporation of the solvent. Tetraethyl orthosilicate (TEOS) at 98% purity [Aldrich] was used as received. Cyclohexane (C_6H_{12}), chloroform, sulfuric acid (H_2SO_4), hydrochloric acid 32%, and hydrogen peroxide (H_2O_2 30%) were HPLC grade (Frutarom Ltd.). The various molar ratios were prepared by mixing the appropriate amounts of parent solutions of TEOS and TRCDA. The water subphase used in the Langmuir trough was doubly purified by a Barnstead D7382 water purification system (Barnstead Thermolyne Corporation, Dubuque, IA), producing water having 18.3 MΩ cm resistivity. Sigmacote™, colorless solution of a chlorinated organopolysiloxane in heptane was purchased from Aldrich. The bacterial strain used in the experiments was *Salmonella enterica* serovar Typhimurium 1a (strain CS093). The bacteria were grown to saturation at 37 °C and streaked. Bacterial concentrations were determined through absorption at 600 nm on a Jasco V-550 spectrophotometer.

2.2. Film preparation

Films were grown at 15 °C in the air/solution interface. The silicate precursor TEOS was added to a chloroform solution of the diacetylene monomer (20 mM TRCDA). Different mole ratios of TEOS/ PDA were examined. The volume of the diacetylene monomer solution ranged from 10 to 400 μL, while the volume of TEOS ranged from 15 up to 300 μL. The corresponding TEOS/PDA ratios ranged from 1:56 to 1:900.

The solutions were sealed, shaken until homogeneous (less than 1 min) and spread onto the wells of 24-well ELISA plates in which each well had a surface area of 2 cm^2 containing 2 ml of HCl 0.2 M. The films were ultraviolet-irradiated (254 nm, 80 W) for 30 s to produce polydiacetylene (PDA).

Cleaning of glass slides was carried out through dipping in a piranha solution consisting of 70 mL of H_2SO_4 and 30 mL of H_2O_2 for 30 min at 70 °C, followed by sonication in the same solution for 10 min. Following the cleaning procedure, the glass was rinsed thoroughly with pure water and dried at 70 °C, subsequently immersed in a Sigmacote™ solution overnight (designed to deposit a hydrophobic surface upon the glass). The treated glass slides were then rinsed with cyclohexane to remove any non-covalently bound molecules. The silica/PDA films were transferred horizontally onto the hydrophobic glass (Langmuir–Schaeffer method).

2.3. Surface pressure/area isotherms

All surface pressure/area isotherms were measured with a computerized Langmuir trough manufactured by NIMA TR516 (Nima technology Ltd., Coventry, UK). The surface pressure was monitored using a 1-cm wide filter paper as a Wilhelmy plate. The experiments were carried out at temperatures of 18 °C using a temperature-controlled Teflon barostat. For the TRCDA isotherm experiments, 50 μL of 2 mM TRCDA in chloroform was spread on the HCl 0.2 M subphase and equilibrated for 15 min, allowing for solvent evaporation prior to compression. For the TRCDA and TEOS isotherm experiments, 30 μL of 2 mM TRCDA and 3 μL of 4.5 M TEOS were mixed and spread on the HCl 0.2 M subphase and equilibrated for 15 min, allowing for solvent evaporation prior to compression.

2.4. Brewster angle microscopy (BAM)

A Brewster angle microscope (NFT GmbH, Gottingen, Germany) mounted on a Langmuir film balance was used to observe the microscopic structures *in situ*. The light source of the BAM was a frequency-doubled Nd/YAG laser with a wavelength of 532 nm and 20–70 mW primary output power in a collimated beam. The BAM images were recorded with a CCD camera. The scanner objective was a Nikon superlong working distance objective with nominal 10 magnification and a diffraction limited lateral resolution of 2 μm. The images were corrected to eliminate side ratio distortion originating from a non-perpendicular line of vision of the microscope.

2.5. Scanning white light interference (SWLI) microscopy

SWLI microscope (New View 200, Zygo, USA) was used to characterize the film surface and thickness using a 50× Mirau objective NA 0.65. The image sizes were 240 × 320 pixels with a pixel size from $(0.9\ \mu m)^2$ to $(0.22\ \mu m)^2$, depending on the zoom.

2.6. Scanning electron microscopy (SEM)

For SEM measurements, films were transferred horizontally onto hydrophobic glass. SEM images were recorded on a Jeol JSM-7400F Scanning electron microscope (JEOL LTD, Tokyo, Japan).

2.7. Fourier-transform infrared (FTIR) microscopy

Silica/PDA samples were transferred onto gold-coated glass, and the FTIR spectrum was collected with a Nicolet iN10 FTIR microscope MX spectrometer (Thermo Scientific) fitted with a narrowband liquid nitrogen cooled MCT detector. The microscope was operated in the reflectance mode. In all cases, the incident infrared beam was focused at a sample surface. All single-beam spectra were measurement against a background recorded from reflectance off a gold-coated disk. Appropriate backgrounds were obtained for each series of measurements. The spectra were recorded in the wave number range of 700–4500 cm^{-1}. Spectral resolution was set at ~4 cm^{-1} over coverage scans 16 scans. The FTIR data were collected using the OMNIC-Picta software. After collection, the automatic atmospheric suppression (to minimize infrared absorption by CO_2 and water vapor in the ambient air) and baseline correction functions in the OMNIC-Picta software were used. Multicomponent analysis was performed using the OMNIC-Spectra software.

2.8. Fluorescence microscopy

Fluorescence microscopy measurements were carried out on an Olympus I×70 microscope equipped with a Roper Scientific Inc. MicroMAX camera. The experiments employed a narrowband filter cube UPlanFI, excitation 470–490 nm, beam splitter 505 nm, and outgoing filter 510 nm. Images were processed with "WINView" software.

2.9. Ultraviolet–visible (uv–vis) spectroscopy

Uv–vis spectroscopy measurements were carried out using a Jasco V-550 spectrophotometer. The spectra were directly acquired using the silica/TRCDA films transferred to glass after different polymerization times.

2.10. Color scanning and image analysis

One hundred and sixty microliters of *Salmonella enterica* serovar typhimurium 1a were placed on the surfaces of the polymerized

silica/PDA films and incubated at 37 °C for different time periods. Lysogeny broth (LB) medium was used as control. The films were sealed in a Petri dish to minimize evaporation. Following incubation, the solution was removed in order to examine the bacterial count by uv–vis measurements. The dried films were scanned on an Epson 4990 Photo scanner to produce high resolution RGB images. Scanning was carried out by placing the films in a special adaptor and scanning in a transmitted mode at 2400 dpi optical resolution and 24 bit color depth. Quantification of the blue–red color transformations was carried out using digital colorimetric analysis (DCA), carried out by cropping the spots within the film images which the sample volume covered, and application of MATLAB mathematical software for calculating the total intensity and abundance of red pixels on the surface [29].

3. Results and discussion

Preparation of PDA-supported silicate films was carried out through gentle deposition of a film comprising the diacetylene monomer and tetraethyl orthosilicate (TEOS) precursor upon a mildly acidic solution (Fig. 1). The mixed films were incubated for approximately 1 h designed to allow both hydrolysis and condensation of the TEOS subunits, as well as self-assembly of diacetylene multilayers (Fig. 1). This was followed by polymerization of the films through ultraviolet irradiation (254 nm) resulting in a silica/PDA film exhibiting a blue color, corresponding to the conjugated PDA network (Fig. 1). Parameters such as precursor concentrations, mole ratio between the two components, subphase composition, and temperature were optimized to enhance stability and homogeneity of the film and preventing aggregation and/or solubilization of the two building blocks. Specifically, we examined a relatively wide range of TEOS/diacetylene mole ratios—between approximately 50:1 and 1000:1. We observed that mole ratio between the two components had a pronounced effect upon the film homogeneity and uniformity. The optimal ratio selected for the experiments was 225:1 (TEOS/diacetylene), which yielded a stable and homogeneous film appearance, see below.

We applied several analytical techniques to characterize the properties of the TEOS/PDA films, both *in situ* and *ex situ*, particularly aiming to determine whether the two components (diacetylene and silica) interact with each other and mutually affect their film organization. Fig. 2 depicts a comparison between the surface pressure/area compression profiles and microscopic dispersion of TEOS/diacetylene films vs. *pure* diacetylene films at the air/water interface. Fig. 2 demonstrates that the surface pressure/area isotherm of the TEOS/diacetylene mixture appears markedly different than the isotherm of pure diacetylene, most likely reflecting the incorporation of the quaternary silicates within the diacetylene framework thereby modulating the film compression properties. Specifically, the mixed TEOS/diacetylene film (Fig. 2A) exhibits a fluid phase and subsequent liquid-expanded/liquid-condensed phase transition at around 10 mN/m—significantly *greater* molecular areas compared to the film of pure diacetylene (Fig. 2B). The recording of a phase transition in the isotherm in Fig. 2A indicates that the presence of TEOS did not disrupt the pressure-induced reorganization of the diacetylene monomers at the air/water interface. However, the higher molecular surface areas apparent in the isotherm are indicative for the inclusion of the TEOS units within the diacetylene film.

The Brewster angle microscopy (BAM) images shown in the insets in Fig. 2 further highlight the different organization of the mixed TEOS/diacetylene films vs *pure* diacetylene. The bright areas in the BAM images correspond to the condensed diacetylene domains [30]. However, both the *shapes* and *distribution* of the diacetylene domains in the two types of films appeared different. Specifically, while intriguing dendritic domains are apparent in the TEOS/diacetylene film, particularly in high surface pressure (Fig. 2A), the pure diacetylene film exhibits a less-ordered condensed domain appearance (Fig. 2B). The BAM results in Fig. 2 thus demonstrate that the inclusion of TEOS modulates the overall film microstructure.

Langmuir diacetylene films are known to undergo photopolymerization and chromatic transformations at the air/water interface induced through uv irradiation (254 nm) [31]. Specifically, previous reports have demonstrated that uv-induced ene–yne conjugation of diacetylene films *in situ* (e.g., at the air/water interface) produces the *blue* polydiacetylene (PDA) phase, which subsequently transforms upon extended irradiation into the *red* polymer phase [32]. Fig. 3 examines whether the inclusion of the TEOS units within the Langmuir TEOS/diacetylene films interferes with the irradiation/polymerization process of the PDA matrix.

Fig. 3A depicts a graph of the time evolution of the visible emission peak at 640 nm (corresponding to the *blue phase* of PDA, blue line in Fig. 3A) and 500 nm (corresponding to the *red phase*, red line in Fig. 3A), respectively, induced upon continuous irradiation of the film at 254 nm. The colorimetric transformations depicted in Fig. 3A confirm that the PDA matrix retains its chromatic properties even in the mixed silica/PDA film: Initially, the increase in intensity of the peak at 640 nm reflects the formation of blue (polymerized) PDA domains. The subsequent *decrease* in the blue peak intensity and simultaneous *increase* of red signal at 500 nm following longer irradiation of the film underlie the transformation into the *red* PDA matrix, expected upon extended uv irradiation [32,33].

Fig. 3B presents camera images of PDA-containing films assembled at the air/water interface. Specifically, a TEOS/PDA film (225:1 mol ratio) exhibits a smooth, blue appearance following polymerization at the air/water interface (Fig. 3B,i). Other TEOS/

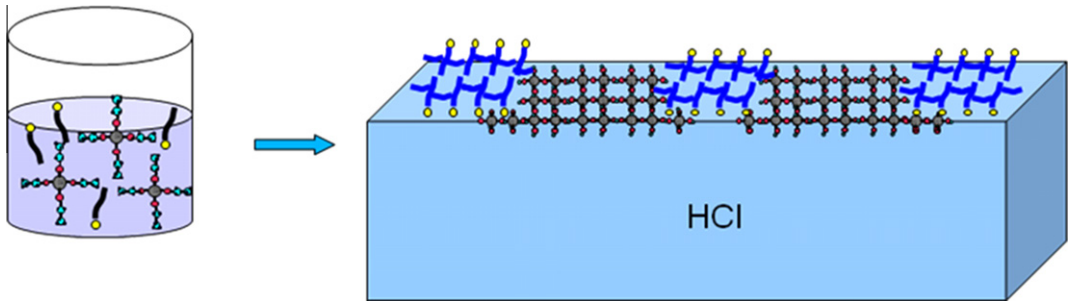

Fig. 1. Construction of silica/PDA films at the air/water interface. The monomer precursors TEOS (cross-shaped molecule) and diacetylene (single chain) were first dissolved in chloroform (left) and deposited upon a mildly acidic solution (right). Following hydrolysis and uv irradiation (254 nm), a blue transparent film is formed comprising the polydiacetylene (PDA) network (blue) interspersed within the silica matrix (black "necklace" structure). (For interpretation of the references to color in this figure legend, the reader is referred to the web version of this article.)

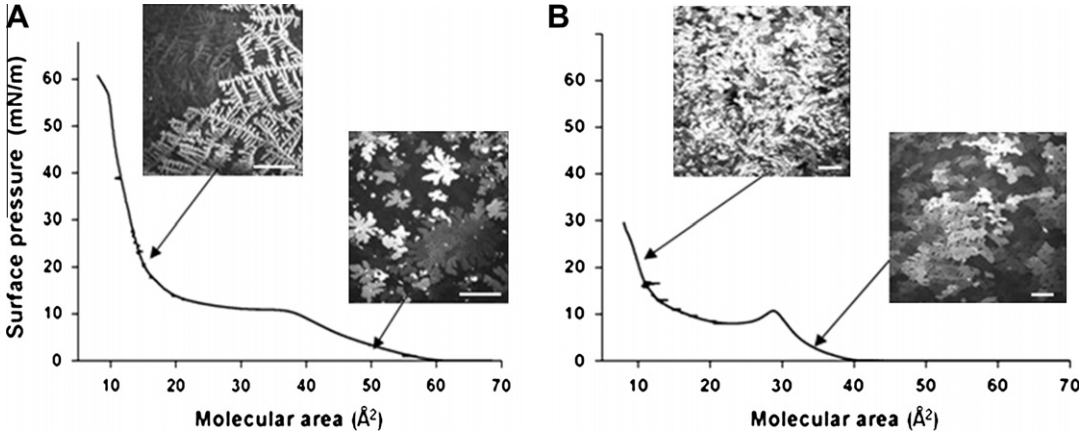

Fig. 2. Film compression at the air/water interface. Surface pressure/area isotherms and Brewster angle microscopy (BAM) images (insets) of a diacetylene/TEOS film (A) and pure diacetylene film (B). Bars correspond to 100 μm.

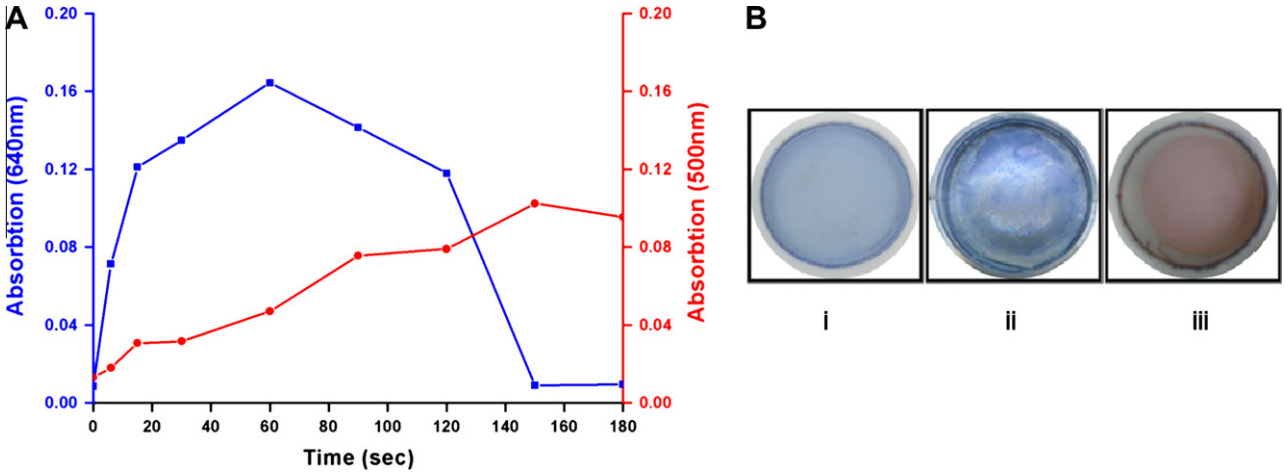

Fig. 3. Colorimetric transformation of the TEOS/diacetylene film at the air/water interface. (A) Intensities of the peaks at 640 nm (corresponding to the blue PDA phase) and 500 nm (corresponding to the red phase) in the visible spectrum following uv irradiation of the film. (B) Camera images of PDA films produced at the air/water interface within wells of a 24-well plate. (i) Blue (as-polymerized) TEOS/PDA (225:1 mol ratio); (ii) pure PDA; (iii) red TEOS/PDA formed through extended uv irradiation. (For interpretation of the references to color in this figure legend, the reader is referred to the web version of this article.)

PDA ratios that were examined exhibited inhomogeneous gelation and non-uniform appearance of the blue PDA color throughout the film. Indeed, the *pure* diacetylene film in Fig. 3B,ii (produced at a similar surface pressure as the silica/PDA film) displays an inhomogeneous surface with abundant aggregates. Following extended longer uv irradiation time, the blue silica/PDA film transforms into the red phase while retaining the homogeneous appearance (Fig. 3B,iii). Overall, the camera pictures in Fig. 3B indicate that the intercalation of TEOS within the PDA gave rise to a homogeneous film exhibiting a smoother visual appearance.

The polymerized silica/PDA films can be transferred from the air/water interface onto solid substrates for further characterization and practical applications. Figs. 4–6 present experimental data designed to characterize the properties of the films *ex situ*, particularly with regard to the molecular organization of the silicate and PDA components. Fig. 4 depicts a scanning white light interference (SWLI) microscopy analysis of a silica/PDA film transferred from the air/water interface onto glass. SWLI microscopy facilitates a topographical examination and vertical resolution at a nanometer scale of thin films [34]. Fig. 4A shows the SWLI microscope image of a film in which intersecting scratches were made with a sharp object, designed to remove parts of the film in order to probe its thickness and topography. Specifically, the height profile in Fig. 4B indicates a relatively uniform film exhibiting thickness of around 220 nm.

A closer investigation of the silica/PDA film surface is facilitated through scanning electron microscopy (SEM) experiments (Fig. 5). Fig. 5 compares the surface morphology of a silica/PDA film and a pure PDA film, respectively, prepared at the air/water interface at the same surface pressure and transferred onto solid substrates. The SEM image recorded for the mixed silica/PDA film in Fig. 5A shows an abundance of elongated irregularly shaped darker domains, ascribed to the PDA units [24]. The SEM data clearly show, however, that the morphology of the mixed TEOS/PDA film is significantly different than the pure PDA film, which exhibits larger and much more dispersed PDA domains (Fig. 5B). The pronounced difference between the PDA domain structure and distribution in the silica/PDA film in comparison with pure PDA reflects the effect of the silica matrix upon the film properties, consistent with the *in situ* characterization data presented in Figs. 2 and 3, above. Importantly, the much smaller empty spaces in the silica/PDA film (Fig. 5A) compared to pure PDA (Fig. 5B) most likely correspond to the greater stability and uniformity of the mixed film.

Fourier-transform infrared (FTIR) microscopy data in Fig. 6 provide further information on the structural elements present in the films. Fig. 6 (right) depicts a two-dimensional FTIR microscopy

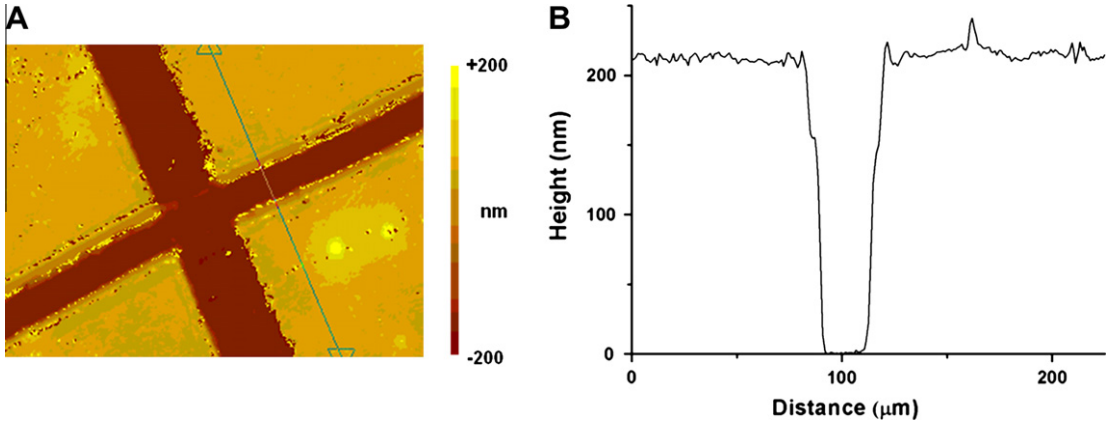

Fig. 4. Macroscopic properties of silica/PDA films. Left: A scanning white light interference (SWLI) microscopy image of a silica/PDA film transferred onto a solid substrate and scratched by a sharp object in order to evaluate film thickness and uniformity. Right: the height profile of the film as determined from the SWLI image (straight line for which the height was recorded is shown in black in the image).

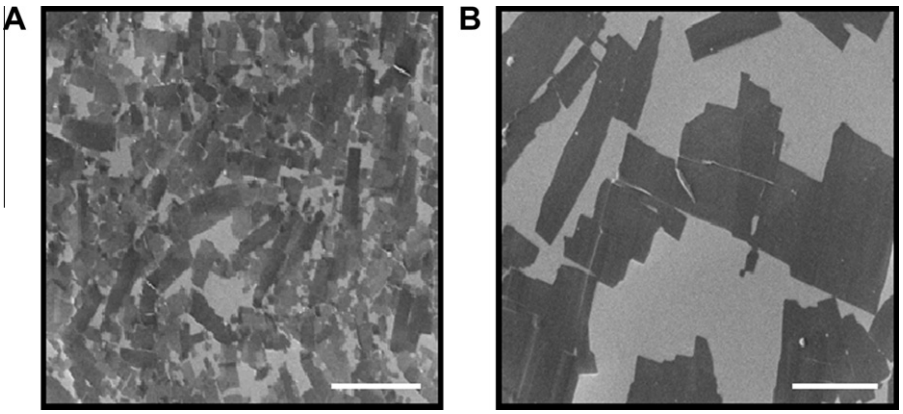

Fig. 5. Surface morphology of silica/PDA films transferred from the air/water interface. Scanning electron microscopy (SEM) images of (A) silica/PDA film and (B) pure PDA film. Both films were prepared at the same surface pressure of ~20 mN/m. Bars correspond to 10 μm.

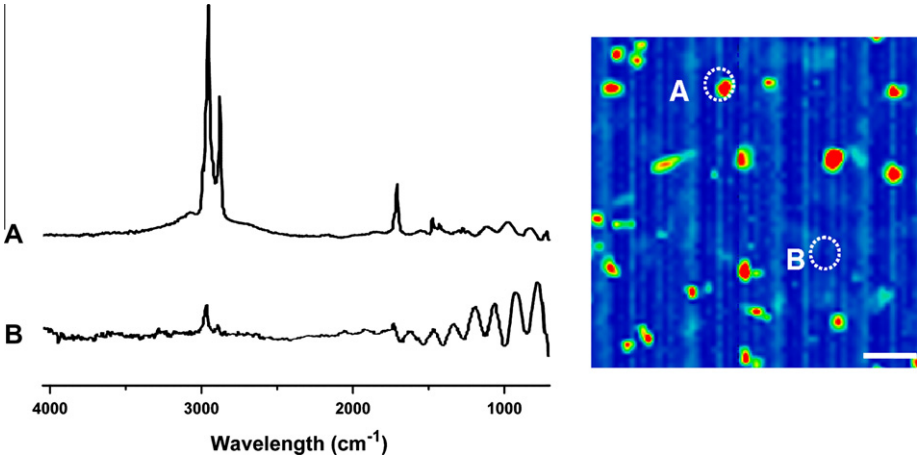

Fig. 6. FTIR microscopy of a silica/PDA film. Right: unvaried map of the sample based upon the intensity of the 2920 cm^{-1} band (scale bar 250 μm). (A) and (B) depict the FTIR spectra recorded in the indicated regions in the film.

map (based upon the carbon 2920 cm^{-1} band) acquired from a representative film area. The FTIR spectra in Fig. 6A and B reveal the structural units within the areas indicated by the small circles in the microscopy map. Specifically, the FTIR spectrum in Fig. 6A highlights the prominent PDA-associated band at around 2800 cm^{-1} and 1500 cm^{-1} (C–X, in which X corresponds to C, O, or H) [35] as well as the presence of silica peaks below 1500 cm^{-1}. Vibration bands corresponding to both PDA and the silica matrices are also clearly apparent in other areas (Fig. 6B). Overall, the FTIR spectra in Fig. 6A and B confirm that polymerized TEOS and PDA did not

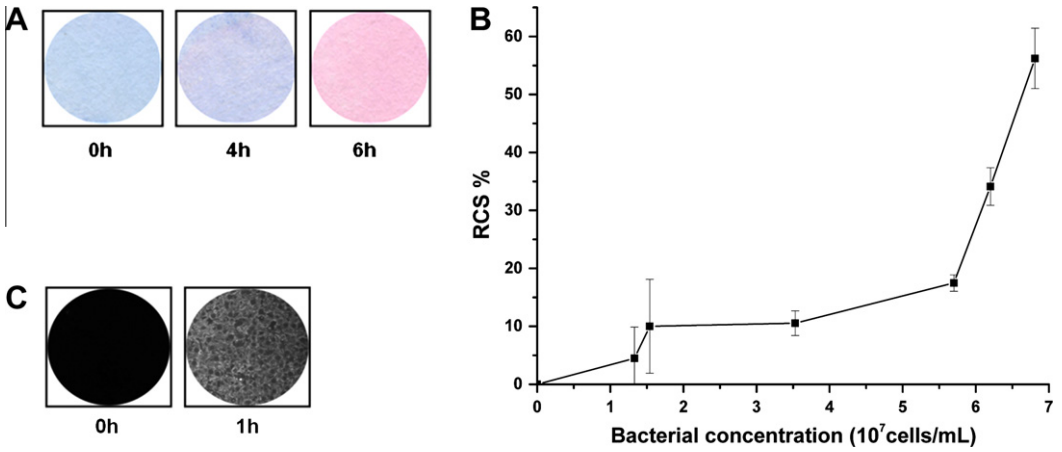

Fig. 7. Chromatic detection of bacteria by silica/PDA films. (A) Wells within a multiwall plate depicting color transformations of the film following incubation with proliferating bacteria (times indicated correspond to incubation periods following spiking with bacteria). (B) Quantitative colorimetric transformation (%RCS) [29] of the silica/PDA film in response to bacterial proliferation. (C) Fluorescence microscopy images depicting bacterially induced fluorescence (times indicated correspond to incubation periods following spiking with bacteria).

form separate regions within the films, but rather exhibited interspersed microscopic domains on a submillimeter scale.

The new silica/PDA film assembly is robust, stable, and could constitute a platform for varied biosensing applications. As an example, we present the utilization of silica/PDA films for bacterial detection (Fig. 7). Previous studies have shown that lipid/PDA vesicles incorporated within agar matrixes can be employed for reporting on bacterial proliferation through colorimetric transitions of PDA [36]. In such systems, PDA undergoes blue–red transformations following interactions with bacterially secreted species [37]. The data presented in Fig. 7 demonstrate that the silica/PDA films can be also employed for monitoring bacterial growth *in situ*.

Fig. 7 presents the results of an experiment in which a glass-supported silica/PDA film was placed in a growth medium (Lysogeny broth, LB) spiked with *Salmonella typhimurium* bacterial cells. Fig. 7A depicts scanned images of the film recorded at different times after spiking the solution with bacteria (initial concentration of approximately 10^7 cells/mL). Fig. 7A clearly shows that the silica/PDA film underwent a gradual blue–red transformation induced by the proliferating bacteria. The colorimetric transformations within the silica/PDA films can be quantified by a conventional desktop scanner and a simple image analysis algorithm [29]. The technique relies upon summation of both the *number* and the *relative intensities* of the red pixels (corresponding to PDA domains that underwent the blue–red transition) in the scanned film images (such as the ones shown in Fig. 7A) [29]. Fig. 7B depicts the dose–response curve quantitatively relating the blue–red transformations of the silica/PDA film to the bacterial concentrations in the medium. Importantly, the *Y* axis values in Fig. 7B correspond to the *net color change*, that is, following subtraction of the residual (background) color change induced by the growth medium and temperature. The colorimetric dose–response curve in Fig. 7B clearly correlates the colorimetric transformations in the silica/PDA film with bacterial proliferation.

The *fluorescence* properties of PDA facilitate enhanced sensitivity for bacterial detection using the silica/PDA films (Fig. 7C). Fig. 7C shows fluorescence microscopy images, demonstrating that the film produced discernable fluorescence emission within an hour after placing the film in a solution containing approximately 10^6 bacterial cells/mL (same spiking as in Fig. 7A). The chromatic transformations of the silica/PDA films depicted in Fig. 7, the versatility of detection methods and film configurations (e.g., the use of a multiwall plate), and sensitivity of the platform point to the potential of the technology for biosensing applications.

4. Conclusions

This work describes the construction of thin chromatic films comprising silica and polydiacetylene, assembled together at the air/water interface. The films can be polymerized *in situ* and subsequently transferred onto solid substrates on which they can be implemented as useful sensing platforms. The contribution of each of the two components is important for film assembly and properties. The *PDA matrix* functions as the surfactant component, designed to facilitate the formation of the free-standing silica film; the amphiphilic diacetylene network in the system depicted in this work is essential for stabilization of the thin silica film at the air/water interface. PDA also functions as the chromatic transducer—reporting on the presence of biological analytes (proliferating bacteria in this work) through both blue–red transitions visible to the naked eye as well as fluorescence emission. The *silica network* facilitates a relatively homogeneous distribution and enhanced stabilization of the PDA units within the film. The inherent *transparency* of the gel matrix is an essential characteristic for sensing applications of the new film assembly.

An important issue pertinent to the new film assembly concerns the interactions between the PDA and TEOS constituents, and how such interactions affect the film properties. Indeed, analytical techniques, applied both *in situ* and *ex situ,* indicate that, first, the two components intersperse within the film, and, second, the mixed TEOS/PDA films exhibit distinct properties that were different (and generally superior) compared to the pure components in film configurations. Specifically, TEOS could form thin film at the air/water interface only in the presence of the diacetylene amphiphiles. Furthermore, the silica matrix gave rise to homogeneous morphologies of the mixed films, minimal aggregation of PDA domains, and enhanced sensitivity of PDA toward external stimuli.

The thin silica/PDA films can be employed for varied sensing applications. Fig. 7, for example, demonstrated utilization of the films for bacterial detection. Fig. 7 shows that the detection of bacterial proliferation is accomplished through both visible and fluorescence microscopy analyses. Currently, the PDA/silica film platform is not bacterially specific. However, even as a general (non-specific) bacterial detector, one can see the advantages of the new film system as compared to conventional bacterial detection techniques and potential uses in applications such as monitoring sterile environments (e.g., packaged food, food-processing areas, medical environments, and drinking water) in which reporting upon bacterial proliferation is crucial.

Acknowledgment

We are grateful to Dr. Jurgen Jopp for help with the microscopy experiments.

References

[1] J.C. Diniz da Costa, G.Q. Lu, V. Rudolph, Y.S. Lin, J. Membr. Sci. 198 (2002) 9–21.
[2] T.S. Glazneva, E.V. Rebrov, J.C. Schouten, E.A. Paukshtis, Z.R. Ismagilov, Thin Solid Films 515 (2007) 6391–6394.
[3] S. Angelos, M. Liong, E. Choi, J.I. Zink, Chem. Eng. J. 137 (2008) 4–13.
[4] P.K.H. Ho, D.S. Thomas, R.H. Friend, N. Tessler, Science 285 (1999) 233–236.
[5] M.H. Huang, F. Kartono, B. Dunn, J.I. Zink, Chem. Mater. 14 (2002) 5153–5162.
[6] P.C.A. Alberius, K.L. Frindell, R.C. Hayward, E.J. Kramer, G.D. Stucky, B.F. Chmelka, Chem. Mater. 14 (2002) 3284–3294.
[7] M. Ogawa, N. Masukawa, Microporous Mesoporous Mater. 38 (2000) 35–41.
[8] Y. Hu, A. Bouamrani, E. Tasciotti, L. Li, X. Liu, M. Ferrari, ACS Nano 4 (2010) 439–451.
[9] C. Wu, Y. Yamauchi, T. Ohsuna, K.J. Kuroda, Mater. Chem. 16 (2006) 3091–3098.
[10] S. Besson, C. Ricolleau, T. Gacoin, C. Jacquiod, J. Boilot, Microporous Mesoporous Mater. 60 (2003) 43–49.
[11] N. Nishiyama, S. Tanaka, Y. Egashira, Y. Oku, K. Ueyama, Chem. Mater. 14 (2002) 4229–4234.
[12] J. Zhang, W. Li, X. Meng, L. Wang, L. Zhu, J. Membr. Sci. 222 (2003) 219–224.
[13] I.A. Aksay, M. Trau, S. Manne, I. Honma, N. Yao, L. Zhou, P. Fenter, P.M. Eisenberger, S.M. Gruner, Science 273 (1996) 892–898.
[14] H. Yang, N. Coombs, I. Sokolov, G.A. Ozin, Nature 381 (1996) 589–592.
[15] D.A. Doshi, A. Gibaud, V. Goletto, M. Lu, H. Gerung, B. Ocko, S.M. Han, C.J. Brinker, J. Am. Chem. Soc. 125 (2003) 11646–11655.
[16] K.J. Edler, A. Goldar, T. Brennan, S.J. Roser, Chem. Commun. 2000 (2003) 1724–1725.
[17] C. Fernandez-Martin, S.J. Roser, K.J. Edler, J. Mater. Chem. 18 (2008) 1222–1231.
[18] G.S. Attard, J.C. Glyde, C.G. Göltner, Nature 378 (1995) 366–368.
[19] R.W. Carpick, D.Y. Sasaki, M.S. Marcus, M.A. Eriksson, A.R. Burns, J. Phys.: Condens. Matter 16 (2004) R679–R697.
[20] H. Tamura, N. Mino, K. Ogawa, Thin Solid Films 179 (1989) 33–39.
[21] A. Lio, A. Reichert, D.J. Ahn, J.O. Nagy, M. Salmeron, D.H. Charych, Langmuir 13 (1997) 6524–6532.
[22] U. Jonas, K. Shah, S. Norvez, D.H. Charych, J. Am. Chem. Soc. 121 (1999) 4580–4588.
[23] J.-M. Kim, E.-K. Ji, S.M. Woo, H. Lee, D.J. Ahn, Adv. Mater. 15 (2003) 1118–1121.
[24] J. Lee, O. Yarimaga, C.H. Lee, Y.-K. Choi, J.-M. Kim, Adv. Funct. Mater. 21 (2011) 1032–1039.
[25] Q. Cheng, R.C. Stevens, Adv. Mater. 9 (1997) 481–483.
[26] F. Gaboriaud, R. Golan, R. Volinsky, A. Berman, R. Jelinek, Langmuir 17 (2001) 3651–3657.
[27] D. Meir, L. Silbert, R. Volinsky, S. Kolusheva, I. Weiser, R. Jelinek, J. Appl. Microbiol. 104 (2008) 787–795.
[28] Y. Lu, Y. Yang, A. Sellinger, M. Lu, J. Huang, H. Fan, Nature 410 (2001) 913–917.
[29] R. Volinsky, M. Kliger, T. Sheynis, S. Kolusheva, R. Jelinek, Biosens. Bioelectron. 22 (2007) 3247–3251.
[30] R. Volinsky, F. Gaboriaud, A. Berman, R. Jelinek, J. Phys. Chem. B 106 (2002) 9231–9236.
[31] J.-T. Cho, S.-M. Woo, D.J. Ahn, K.-D. Ahn, H. Lee, J.-M. Kim, Chem. Lett. 32 (2003) 282–283.
[32] D.Y. Sasaki, R.W. Carpick, A.R. Burns, J. Colloid Interface Sci. 229 (2000) 490–496.
[33] Y. Su, React. Funct. Polym. 66 (2006) 967–973.
[34] L. Faget, A. Berman, O. Regev, Thin Solid Films 386 (2001) 6–13.
[35] S.J. Kew, E.A.H. Hall, Anal. Chem. 78 (2006) 2231–2238.
[36] Y. Scindia, L. Silbert, R. Volinsky, S. Kolusheva, R. Jelinek, Langmuir 23 (2007) 4682–4687.
[37] L. Silbert, I. Ben Shlush, E. Israel, A. Porgador, S. Kolusheva, R. Jelinek, Appl. Environ. Microbiol. 72 (2006) 7339–7344.